A simplified thermodynamic effect model for cavitating flow in hot water

IOP Conf. Series: Earth and Environmental Science **240** (2019) 062024 doi:10.1088/1755-1315/240/6/062024

A simplified thermodynamic effect model for cavitating flow in hot water

A D Le[1] and Y Iga[2]

[1] Graduate School of Engineering, Tohoku University, Japan
[2] Institute of Fluid Science, Tohoku University, Japan

E-mail: le@cfs.ifs.tohoku.ac.jp

Abstract. When cavitation occurs, under the evaporation cooling effect, the local temperature decreases, saturated vapor pressure decreases, then cavitation is suppressed. This is known as "thermodynamic effect" of cavitation, which is normally neglected in water cavitation at room temperature. Due to the low liquid-vapor density ratio, the thermodynamic effect becomes much more important and cannot ignore in hot water cavitation. Therefore, in numerical simulation, the thermodynamic effect needs to be taken into account. This study, a simplified thermodynamic model, which has been applied to liquid nitrogen cavitation, combining with our cavitation model is extended to hot water cavitation. The cavitation experiment on a 2-D triangle cylinder in the water at 90^0C is conducted. The temperature depression in cavity under thermodynamic effect is measured by using the thermistor probe. Then, experimental data is used for validating the present simplified thermodynamic model. Furthermore, the present model is extended to cryogenic cavitation. The numerical result shows good agreement in cavity volume and temperature comparison with experiment in the present hot water and cryogenic liquid.

1. Introduction

Cavitation is the formation of vapor phase inner liquid phase when the local pressure decreases to its saturated vapor pressure due to the flow acceleration. Cavitation is the major concern in hydraulic machinery due to the increase in noise, vibration, performance degradation and erosion. It is well known that the thermodynamic effects can significantly suppress the cavity volume. When cavitation occurs, the heat supplied from surrounding liquid is needed for vaporization, hence the liquid temperature is decreased and cavitation is suppressed. Hence, the system performance can be improved. In cavitation research, a number of cavitation experiments have been conducted with water at room temperature, in that the thermodynamics effect is usually neglected. However, in industrial application, the cryogenic liquid (N_2, H_2, etc.), thermal sensitive liquid (R114, etc.) or hot water are the popular working fluids. For those fluids, due to the low liquid-vapor density ratio, the thermodynamic effects of cavitation become much more important and cannot ignore.

Theoretically, the non-dimension temperature depression B-factor [1] commonly uses to estimate the temperature depression due to the thermodynamic effect of cavitation. This factor strongly depends on flow characteristics such as the vapor void fraction, which is unknown. Therefore, the temperature depression cannot be exactly estimated. Therefore, the measurement of temperature depression in cavity is necessary. Hord studied the cavitation in liquid nitrogen and liquid hydrogen on hydrofoil [2]. The pressure and temperature were measured by using pressure transducers and thermocouples on

the body. The analysis showed that the maximum temperature decreases near cavity leading edge and gradually increases along the cavity. Franc et al. [3] measured the temperature depression within the leading edge of cavity in liquid R114 on space inducer. The thermocouples were mounted on the induce blade. They showed that the temperature depression increases when cavitation number decreases. Yamaguchi et al. [4] conducted temperature measurement inside the cavitation on NACA0015 in water with wide range of temperature from room temperature to 80^0C. The temperature depression in supercavitation was obtained by using thermistor probes. As the results, when free stream temperature rose up, the temperature depression increased. The maximum temperature depression is about 0.21^0C in the water temperature of 80^0C and remains constant within cavity volume.

Numerical simulation, the homogeneous model coupled with a thermodynamic effect model is the powerful tool for this purpose. Up to date, several efforts to take account the thermodynamic effects for cavitating flow simulation has been developed. Tsuda et al. [1] introduced a simplest method. Instead of solving an additional energy transport equation, the saturated vapor pressure is modified base on the B-factor theory. This method was success to reproduce the pressure distribution on hydrofoil and venturi nozzle in cryogenic liquid. However, the temperature profile did not observe. Hosangadi et al. [5] and Iga et al. [6] took account the thermodynamics effect by solving an additional energy transport equation. Hosangadi et al. [5] solved the enthalpy conservation equation for mixture and applied to cryogenic liquid cavitation on hydrofoil. Iga et al. [6] solved a total energy conservation equation for the liquid phase. The heat source term, which is the function of latent heat of phase change and mass transfer rate, is added to the energy transport equation. Then the saturated vapor pressure is estimated base on the flow field temperature. However, the temperature distribution could not correctly reproduce in those methods [5]. We [7] simplified the mixture total energy conservation equation in form of mixture temperature equation and applied to the liquid nitrogen cavitation on hydrofoil.

In this study, the experimental study of the thermodynamic effects of cavitation on the 2-D triangle cylinder is conducted in the water at 90^0C. The thermistor probe is used to measure the temperature depression in cavity. Then, the experimental data is used for validating our simplified thermodynamics effect model. Additionally, our cavitation model is extended to cryogenic cavitation.

2. Experimental Setup

The experiment is conducted in the water cavitation tunnel which can operate under high temperature up to 140^0C and high pressure of 0.5MPa as in the Fig 1. The test section geometry is a channel of 30mm height and 20mm width in cross section and 330mm long. The visualization window is made of glass that enables to view the cavitation appearance. The electric heater is used to control the free stream temperature with the accuracy of 0.1^0C. The operating pressure is controlled by pressure tank that connects to the compressor and vacuum chamber. The flow velocity and its distribution were measured with LDA, the detail can refer to the Yamaguchi et al. report [4].

In this study, the 2-D triangle cylinder is designed for cavitation experiment. Two thermistor probes, the NIKKISO N317/BR14KA103K/23300/RPS/3/SP, are inserted from the sidewall to the core of tunnel section with the help of stainless steel pipe of 1.3mm in diameter to prevent the effect of wall and thermal boundary layer on measurement. The detail configuration of test body and thermistor probes show in Fig 1. The first thermistor probe measures the free stream temperature. This thermistor prober is upstream bent parallel to incoming flow. The head of thermistor probe is about 3 mm away the stainless steel pipe. The second thermistor probe measures the temperature inside the cavity and locates at 24mm downstream of test body. The two temperatures are measured simultaneously and are analyzed by digital multi-meter. The expanded uncertainly of the measurement is 0.02K. The influence of thermal entry on the second thermistor probe from sidewall was estimated [4]. The effect of cavitation occurred on stainless steel pipe on the first thermistor probe were analyzed under steady-state heat conduction and heat convection by Fluent 18.0. The result showed that the temperature influence is less than 0.01K. For experiment, the temperature was obtained by averaging 30 seconds of

measurement. The pressure at upstream of the test body is measured by pressure transducer. The pressure and flow rate are measured and are analyzed by Data Logger software.

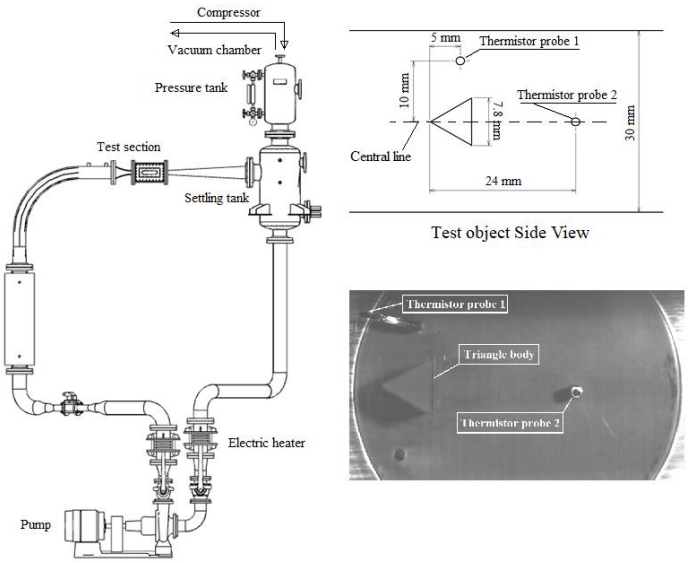

Figure 1. Overview of water cavitation tunnel and the configuration of test object and thermistor probes.

3. Numerical Method

3.1. Simplified thermodynamic model

By assuming the local equilibrium in pressure, temperature and velocity, the set of system equations for the compressible two-phase flow can be rewritten for the mixture in a simple form as for single-phase flow. The transportation equation for vapor mass fraction is derived for the phase change rate. The conservation equation of temperature for mixture phase is derived from the mixture total energy conservation equation [7]. This equation is our simplified thermodynamic model. In that, the source term S_h is the heat source that defines by multiplying the latent heat L of phase change by mass transfer rate. This heat source explicitly appears, then, we can adjust the degree of heat transfer rate to suit the homogeneous model. The governing equations for vapor-liquid two-phase medium in 2-D Cartesian coordinate without turbulence model are expressed as follow:

$$\frac{\partial \mathbf{Q}}{\partial t}+\frac{\partial \mathbf{E}_i-\mathbf{E}_{\mathbf{v}_i}}{\partial x_i}=\mathbf{S}$$

$$\mathbf{Q}=\begin{bmatrix}\rho\\ \rho u_i\\ \rho T\\ \rho Y\end{bmatrix},\quad \mathbf{E}_i=\begin{bmatrix}\rho u_i\\ \rho u_i u_j+\delta_{ij}p\\ \rho u_i T\\ \rho u_i Y\end{bmatrix},\quad \mathbf{E}_{\mathbf{v}_i}=\begin{bmatrix}0\\ \tau_{ij}\\ q_i/c_p\\ 0\end{bmatrix},\quad \mathbf{S}=\mathbf{A}\begin{bmatrix}0\\ 0\\ S_h/c_p\\ m\end{bmatrix} \tag{1}$$

Where ρ, u_i, p, T, Y are the mixture density, velocity components, pressure, temperature and vapor mass fraction, respectively. τ_{ij} and q_i are the viscous shear stress and thermal flux. m is the rate of phase change. The liquid phase is assumed as compressible fluid. The density is estimated by Tammann type equation. The vapor phase is assumed as an ideal gas.

$$\rho_l=\frac{p+p_c}{K_l(T+T_c)},\quad \rho_g=\frac{p}{R_g T} \tag{2}$$

The subscripts l and g denote the liquid and vapor phase. p_c and T_c are the constant for the liquid, respectively. K_l and R_g are the liquid and vapor constant.

The mixture density is linearly expressed from vapor phase and liquid phase density with the local vapor void fraction α:

$$\rho = (1-\alpha)\rho_l + \alpha\rho_g \tag{3}$$

The following relation between vapor void fraction and its mass fraction is obtained:

$$\rho(1-Y) = (1-\alpha)\rho_l, \quad \rho Y = \alpha\rho_g \tag{4}$$

Then, the equation of state, which enclosed the Eq. (1), is derived as:

$$\rho = \frac{p\left(p+p_c\right)}{K_l\left(1-Y\right)p\left(T+T_c\right)+R_g Y\left(p+p_c\right)T} \tag{5}$$

The mixture viscosity [8] is expressed as:

$$\mu = (1-\alpha)(1+2.5\alpha)\mu_l + \alpha\mu_g \tag{6}$$

For present study, two models of heat input by condensation are studied, which are the fully heat input model by Eq. (7) and modified heat input model by Eq. (8).

The fully heat input model:

$$S_h = Lm = L(m^+ + m^-) = Lm^+ + Lm^- = H_e + H_c \tag{7}$$

The modified heat input model:

$$S_h = H_e + 0.8H_c = H_e + H_c^* \tag{8}$$

In that, the latent heat of phase change is defined as:

$$L = h_g - h_l = (c_{pg} - c_{pl})T + h_{0g} - h_{0l}, \quad c_p = Yc_{pg} + (1-Y)c_{pl} \tag{9}$$

c_p, c_{pl} and c_{pg} are the specific heat capacity of the mixture, liquid phase and vapor phase, respectively. h_g and h_l are the specific enthalpy vapor phase and liquid phase. h_{0g} and h_{0l} are the specific enthalpy constant of vapor phase and liquid phase at reference temperature.

3.2. Phase change model

Our cavitation model [9] is chosen for modeling the mass transfer rate. The rate of phase change is derived as below:

$$\begin{aligned} m = m^+ &= C_{a/e}[\alpha(1-\alpha)]^2 \frac{\rho_l}{\rho_g} \frac{\max[0, p_v(T)-p]}{\sqrt{2\pi R_g T}} \\ m = m^- &= C_{a/c}[\alpha(1-\alpha)]^2 \frac{\min[0, p_v(T)-p]}{\sqrt{2\pi R_g T}} \end{aligned} \tag{10}$$

Where, $C_{a/e}$ and $C_{a/c}$ are the empirical constant and has dimension of *1/m*. For the water at room temperature, the value of 0.1 was recommended [9]. The saturated vapor pressure $p_v(T)$ is estimated by using Sugawara equation [10].

3.3. Viscous model

Numerical analysis shown that the numerical solution of cavitation is strongly influenced by the viscous model in boundary layer [5, 6]. Hence, in this study, the laminar simulation and turbulent simulation by Wilcox k-ω turbulence model are performed for the viscous model effect. The detail of k-ω turbulence model can be referred to Wilcox book [11].

3.4. Numerical scheme

Symmetric TVD Maccomack scheme, which bases on the finite difference method, is used for modeling the unsteady cavitating flow. This scheme has second order accuracy in time and space. The TVD scheme can suppress the oscillation near the shock; hence can capture the discontinuity contact in density at the phase change region. The viscous terms in $\mathbf{E}_{vi}$ are discretized by a second-order space-centered scheme. For the turbulent modeling, the scalable wall function is applied at the grid points away the wall. The detail of symmetric TVD Maccormack scheme and the validation can refer to Yee's paper and Le et al. paper [12, 7].

4. Results and Discussion

4.1. Measurement of cavity temperature

In present study, temperature depression inside cavity is measured using thermistor probes. The working fluid is water at temperature of 90^0C. The flow velocity is 6 m/s. The cavitation number is varied by adjusting the tunnel pressure, which defined by Eq. (11).

$$\sigma = \frac{p_{in} - p_v(T)}{0.5\rho U_0^2} \tag{11}$$

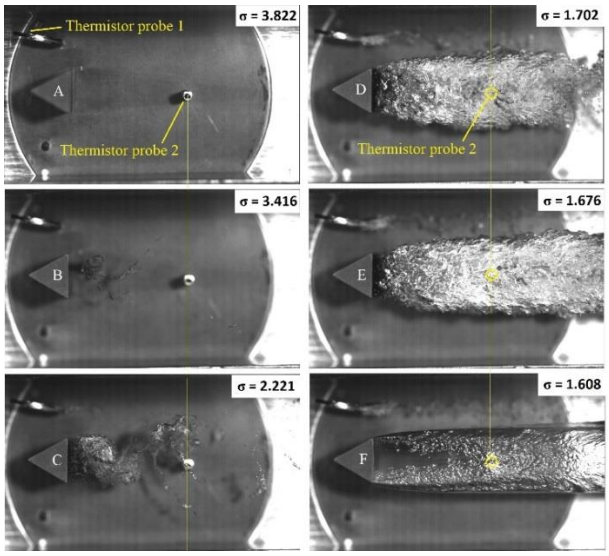

Figure 2. Influence of cavitation number on cavity aspect.

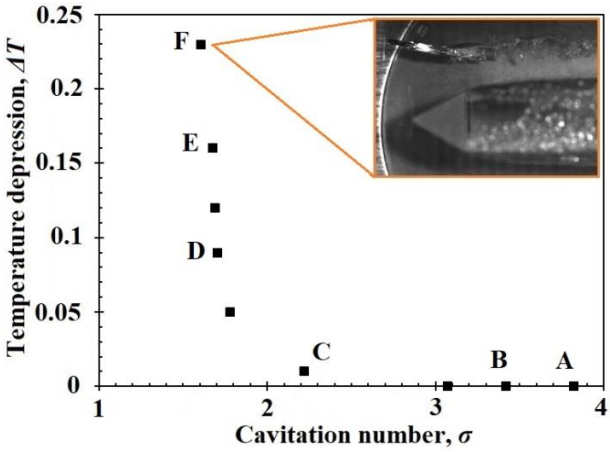

Figure 3. Temperature depression regarding to the cavitaton number

Figure 2 shows the aspect of cavitation on the 2-D triangle cylinder at different cavitation number. Typically, three types of cavitation aspect are visualized from experiment when cavitation number decreases such as the inception-developing cavitation, the developed cavitation and the supercavitation. The picture A, B and C are the inception-developing cavitation. In that, the cavity occurs behind the triangle and does not fully cover the second thermistor probe. The cavity is influenced by Karman vortex in these conditions. Hence, the second thermistor probe is mainly covered by pure water. For developed cavitation as in picture D and E, the cavity reaches and fully covers the second thermistor probe. For this type of cavitation, from the visualization, the thermistor probe is covered by both cavity and pure water cyclically. In picture F, the supercavitation is visualized. The second thermistor probe is always covered by the gaseous cavitation. The influence of cavitation number on temperature depression is shown in figure 3. It can be seen that the cavitation does not occur at the head of first thermistor probe in supercavitation condition. The temperature depression increases as cavitation number decreases from non-cavitation to supercavitation, which corresponds to the three type of cavitation aspects above. This is consistent with Yamaguchi et al. results [4]. In the inception-developing cavitation, the cavity does not reach the second thermistor probe. Then, the different temperature of thermistor probes are relative small. The temperature depression dramatically increases in the developed cavitation condition. In supercavitation condition, the temperature depression is relatively high comparison with the other condition because the second thermistor probe is always covered by cavitation. The temperature depression rises to the maximum of 0.225^0C.

4.2. Numerical results

4.2.1 Hot water cavitation, The O-grid topology is generated over the triangle as in figure 4. The grid is orthogonal and is clustered to the body surface. The cavitation experiment at room temperature and three difference grids, which are 161 x 120 (coarse mesh), 241 x 180 (moderate mesh) and 241 x 200 (fine mesh), are performed for grid sensitive study with laminar boundary layer assuming. The result of moderate mesh and fine mesh show small difference by comparing the time-averaged vapor void fraction distribution. Therefore, the moderate mesh (241 x 180) is used for all simulations.

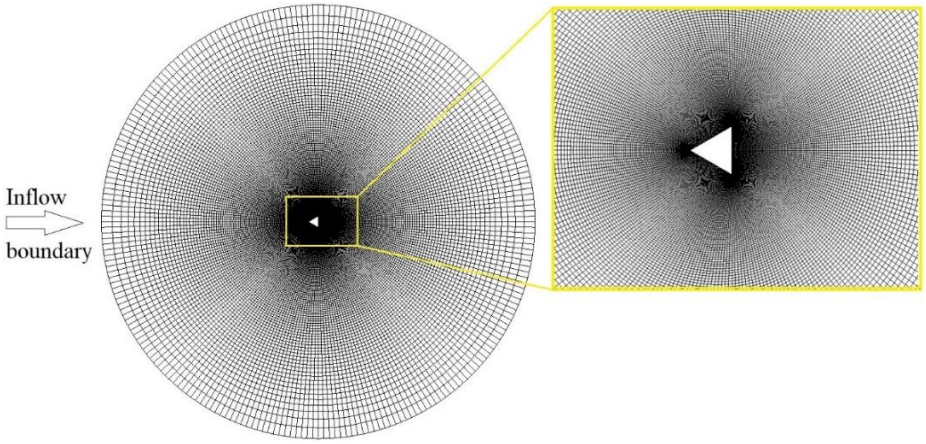

Figure 4. The numerical domain and grid on a 2D triangle cylinder.

The experimental condition of σ = 1.689 and T_0 = 90^0C is selected for validation of our simplified thermodynamics model, which belongs to the developed cavitation aspect. It is well known that the solution of cavitation problem is strongly influence by coefficient constant. Saito et al. suggested the value of 0.1 for two empirical constants $C_{a/e}$, $C_{a/c}$ for the water cavitating flow on NACA0015 at 293K [9]. The empirical constant (0.01) was used by Iga et. al. for the hot water and liquid nitrogen problem [8]. Hence, for present hot water study, at first, the effect of those empirical constant on the numerical simulation of cavity volume and temperature are studied. Four sets of coefficient of 0.1, 1, 10 and 100 are performed. The fully heat input model by Eq.(7) is used in the simulation. Then, the modified heat input by condensation model is validated. The constant uniform velocity U_0, temperature T_0 are specified at inlet boundary. For external flow, typically small value of turbulent intensity and turbulent viscosity ratio are specified, which are 1% and 10 in this study, respectively. The initial void fraction is 0.01. At outlet boundary, static pressure is specified. No-slip condition is applied on triangle body.

Figure 5 shows the time-averaged vapor void fraction and temperature distribution with different coefficient parameters comparison with the averaged image of experiment. The laminar simulation is performed. The empirical constant of 0.1 ~ 10 show a nearly similar cavity volume comparison with experiment. For $C_{a/c} = C_{a/e} = 100$, the cavity aspect differs from the other results and is shorter than experiment. On the other hand, the temperature shows similarity distribution by all coefficient parameters. In all cases, minimum temperature is not in the central of cavity but in the symmetric region from the triangle central line. This is because the re-entrance flow occurs by the effect of two vortex structure and moves to upstream. Then two main cavities is formed in both sides of the central line as in figure 7. This behaviour consists with the visualization experiment. The minimum temperature is about 362.7K. By changing the empirical constant form 0.1 to 100, the minimum temperature region increases. Table 1 is the comparison of temperature depression between numerical simulations by different empirical constant and experiment data. In that, the $C_{a/c} = C_{a/e} = 0.1$, the temperature depression is estimated about 0.127, which best agrees with experiment data with error of 6.67%. Hence, the empirical constant of 0.1 is used for further simulation.

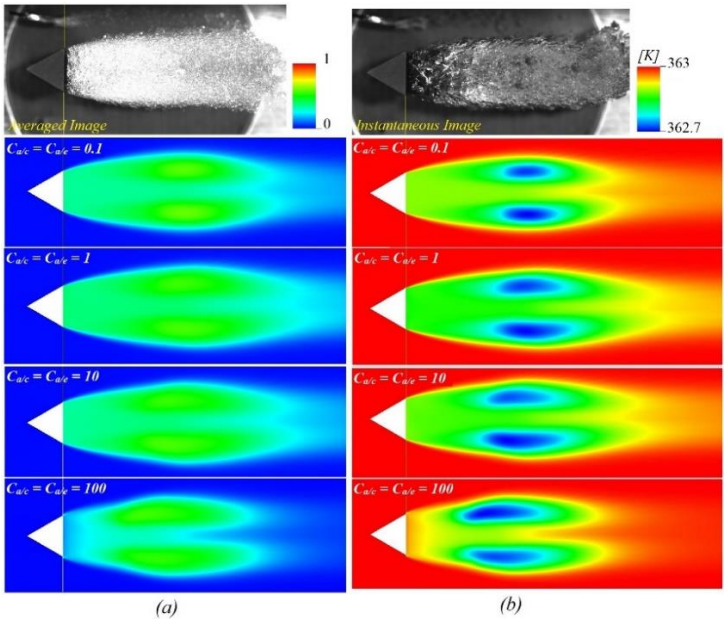

Figure 5. Time-averaged void fraction (a) and temperature distribution (b) of four sets of empirical constant by fully heat input model (σ = 1.689, T_0 = 90^{0}C, U_0 = 6 m/s).

Table 1. Comparison of estimation of temperature depression by different empirical constants in fully heat input model.

σ = 1.689, T_0 = 90^{0}C, U_0 = 6 m/s				
Coefficients	**ΔT_{sim} [^{0}C]**	**ΔT_{exp} [^{0}C]**	**Error [%]**	
$C_{a/c} = C_{a/e} = 0.1$	0.126	0.12	5	Modified heat input model
$C_{a/c} = C_{a/e} = 0.1$	0.127	0.12	5.83	Fully heat input model
$C_{a/c} = C_{a/e} = 1$	0.146	0.12	17.8	
$C_{a/c} = C_{a/e} = 10$	0.142	0.12	17.5	
$C_{a/c} = C_{a/e} = 100$	0.091	0.12	24.2	

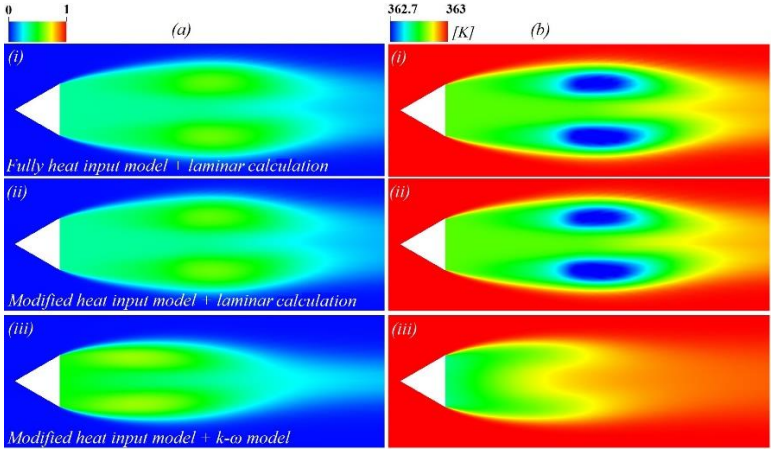

Figure 6. Time-averaged vapor void fraction (a) and temperature (b) between fully heat input by condensation model and modify model in laminar and turbulent viscous model.

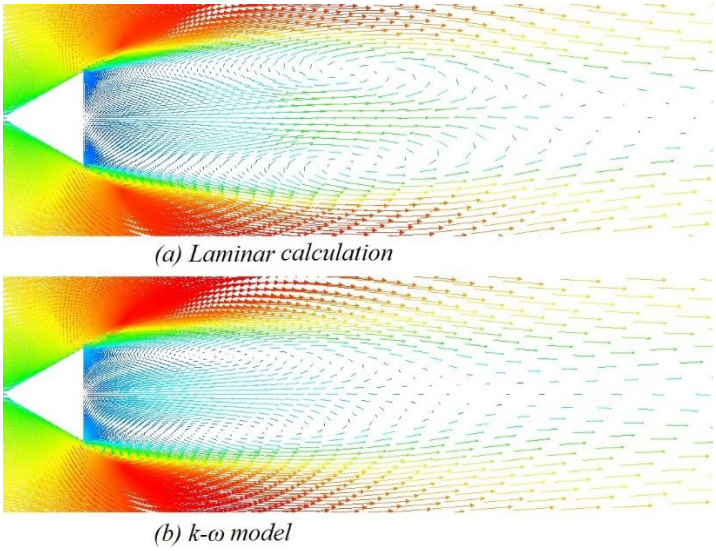

Figure 7. Velocity vector in laminar and turbulent simulation.

Watanabe et al. studied the thermodynamic effects on unsteady cavitating flow and cavitation instability. In his method, the heat flux by condensation was neglected in the downstream of the cavity trailing edge [13]. We performed the study of effect of heat input by condensation model on the numerical simulation of inviscid cavitation on hydrofoil in liquid nitrogen [7]. The results indicated that the fully heat input by condensation causes the temperature over-estimation on hydrofoil surface in downstream region. A modification of heat input of condensation model was suggested that improves the temperature profile comparison with experiment [7]. In the present study, the modified heat input model is applied to the hot water cavitation. Figure 6 is the quantitatively comparison of time-averaged vapor volume fraction and temperature between the fully heat input model and the modified heat input model with (*iii*) and without (*i, ii*) turbulence model. The nearly similarity of vapor volume and temperature distribution is reproduced by two models in case of laminar calculation. Comparing to the error of 5.83% by fully heat input model, the temperature depression of 0.126^0C is obtained by the modified heat input model, which corresponds to the error of 5% as in Table 1. However, by using k-ω turbulent model, the cavity shape and temperature distribution look difference comparison with other models. The maximum temperature depression is 0.2^0C near triangle edge and 0.07^0C at the measurement point, which is completely underestimation. This is because the re-entrant flow is largely suppressed by using k-ω turbulence model as shown in Fig 7. Therefore, the modification of turbulent viscosity may be needed in order to reproduce the re-entrance flow, which does not investigate in this study. It indicates that the modification of heat input by condensation is applicable for not only liquid nitrogen but also for the hot water.

4.2.2 Extension to cryogenic cavitation, Next, the cavitation in liquid hydrogen are investigated by our simplified thermodynamic model with the modified heat input model. The experiment run 247B in liquid hydrogen is performed [2]. The experiment conditions show in Table 2. At inlet, the uniform velocity U_0, temperature T_0, initial vapor void fraction of 1%, turbulence intensity of 5% and turbulence viscous ratio of 1000 are specified [14]. Static pressure is specified at outlet boundary. No-slip condition is applied at wall. The numerical analysis domain can be referred in our paper [7]. Through numerical analysis, the value of $C_{a/e}$ and $C_{a/c}$ are chosen as 50000 and 150000 for liquid hydrogen. Figure 8 shows the time-averaged pressure and temperature distribution on hydrofoil in run 247B comparison with experiment (at the top) and reference result by Hosangadi et al. [5] (at the bottom). The pressure profile agrees well comparison with experiment data. That correspond the numerical cavity length of 1.72cm, which are close to the experiment data. The estimation temperature at the cavity leading edge shows the good comparison with experiment data. Along the cavity length,

the temperature recovery rate satisfies well with temperature profile by experiment, especially in the near cavity trailing edge comparison with Hosangdi's data.

Table 2. Experiment conditions of cryogenic cavitation on hydrofoil [2].

Working Fluid	Run	T_0 [K]	P_0 [kPa]	U_0 [m/s]	σ	l_{cav} [cm]
LH2	247B	20.69	366.8	65.2	1.68	1.52

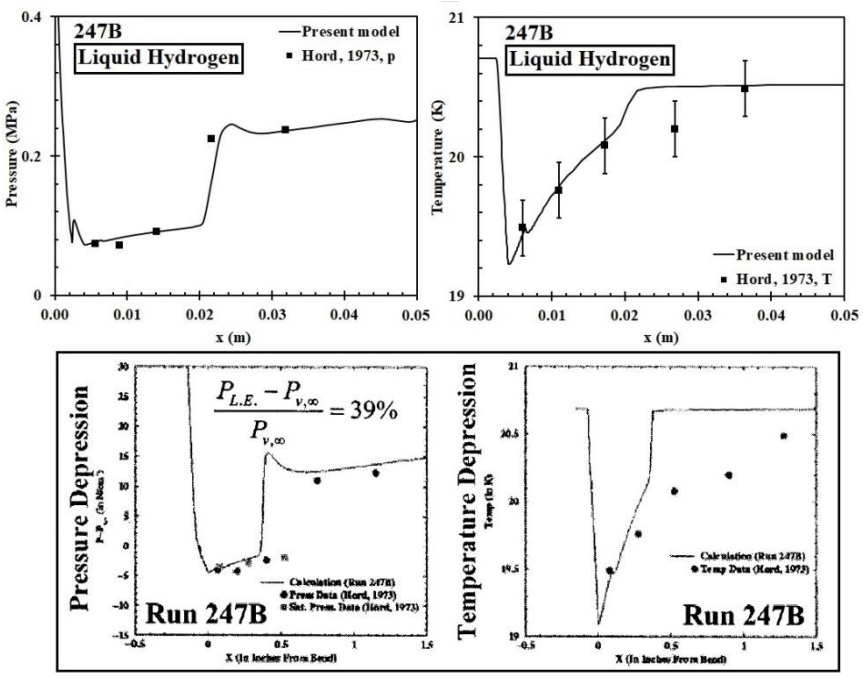

Figure 8. Time-averaged pressure and temperature profile on hydrofoil in liquid hydrogen cavitation by present modified heat input model (upper) and Hosangadi's results [5] (lower).

5. Conclusion

In this paper, the thermodynamic effect of cavitation on 2-D triangle cylinder in hot water was studied by both experiment and numerical simulation. The main results are summarized below:

(a) Through experiment, the temperature depression in cavity was measured by using thermistor probe. The temperature depression increases when cavitation number decreases. The maximum temperature depression is 0.225^0C in case of supercavitation in the measurement point, which is in central line downstream of triangle cylinder.

(b) Our cavitation model combining with our simplified thermodynamic model has been succeeded to simulate the hot water cavitation on 2-D triangle cylinder. Empirical constant in phase change model is suggested for hot water and liquid hydrogen cavitation.

(c) The result by modify heat input by condensation shown good agreements comparison with the present experiment data in hot water. The agreement is also shown in liquid hydrogen cavitation. It indicates that the present simplified thermodynamic model is applicable for simulating thermodynamic effects of cavitation.

Acknowledgment

The authors would like to thank Prof. Satoshi Watanabe at Kyushu University for his valuable discussions on the derivation of present thermodynamic effect model.

References

[1] Tsuda S, Tani N and Yamanishi N 2012 Development and Validation of a Reduced Critical Radius Model for Cryogenic Cavitation *ASME J. Fluids Eng*. Vol. **134**, pp. 051301-1-9.
[2] Hord J 1973 *Cavitation in Liquid Cryogens. II—Hydrofoil* NASA Report No. **CR-2156**.
[3] Franc J-P, Boitel G, Riondet M, Janson E, Ramina P and Rebattet C 2010 Thermodynamic Effect on a Cavitating Inducer-Part II: On-Board Measurements of Temperature Depression Within Leading Edge Cavities *ASME J. Fluids Eng*. Vol. **132** 021304-1.
[4] Yamaguchi Y and Iga Y 2014 *Thermodynamic Effect on Cavitation in High Temperature Water* ASME 2014 4th Join US-European Fluids Engineering Division Summer Meeting and 11th International Conference on Nanochannels, Microchannels, and Minichannels, Chicago, USA.
[5] Hosangadi A and Ahuja V 2005 Numerical study of cavitation in cryogenic fluids *ASME J Fluids Eng-Trans ASME* **127**(2): 267－281.
[6] Iga Y, Ochiai N, Yoshida Y and Ikohagi T 2009 *Numerical Investigation of Thermodynamic Effect on Unsteady Cavitation in Cascade* Proc. of 7th Int. Symposium on Cavitation CAV2009 paper No.**78**.
[7] Le A D and Iga Y 2017 *Simplified Modeling of Cavitating Flow with Thermodynamic Effects for Homogeneous Model* ISROMAC17, Hawaii, Maui, December 16-21.
[8] Beattie D R H and Whally P B 1982 A Simple Two-Phase Frictional Pressure Drop Calculation Method *Int. J. Multiphase Flow* Vol. **8** No. 1 pp. 83-87.
[9] Saito Y, Takami R, Nakamori I and Ikohagi T 2007 Numerical Analysis of Unsteady Behavior of Clound Cavitation around a NACA0015 Foil *Comput. Mech.* **40**:85-96.
[10] Sugawara S 1993 New Steam Table *Journal of the Japan Society of Mechanical Engineers* Vol.35 No.**186** pp.999-1004 (in Japanese).
[11] Wilcox D C 1993 *Turbulence Modeling for CFD* DCW Industries, Inc ISBN **0-9636051-0-0**
[12] Yee H C 1987 *Upwind and Symmetric Shock - Capturing Schemes* NASA Technical Memorandum 89464.
[13] Watanabe S, Hidaka T, Horiguchi H, Furukawa A and Tsujimoto Y 2006 Steady Analysis of the Thermodynamic Effects of Partial Cavitation Using the Singularity Method *ASME J. Fluid Engineering* **129**(2): 121-127.
[14] Tseng C-C and Shyy W 2009 *Turbulence Modeling for Isothermal and Cryogenic Cavitation* 47th AIAA Aerospace Sciences Meeting Including The New Horizons Forum and Aerospace Exposition 5-8 January Orlando Florida.